Influence of the Stabilization Temperature on Textural and Structural Features and Ion Release in $SiO_2-CaO-P_2O_5$ Sol−Gel Glasses

D. Arcos,[†] D. C. Greenspan,[‡] and M. Vallet-Regí*,[†]

Dpto. de Química Inorgánica y Bioinorgánica, Ftad. de Farmacia, UCM, 28040 Madrid, Spain, and USBiomaterials Corporation, Alachua, Florida 32615

Received May 16, 2001. Revised Manuscript Received January 22, 2002

Two different $SiO_2-CaO-P_2O_5$ glasses have been synthesized by the sol−gel method, and the stabilization of the gel glasses was carried out at temperatures between 500 and 800 °C. The different thermal treatments lead to changes in the structural and textural properties. When the glasses were soaked in a buffered solution, the activation energy for calcium release increased with the stabilization temperature. The changes in the silicon release were found to be closely related to the changes in textural properties and network density. The evolution of such changes depended on the chemical composition of the glasses. As an assumption, the differences in behavior between both compositions can be explained in terms of the chemical structure of the glasses. The Ca/Si ratio appears to play a fundamental role in this behavior.

Introduction

Bioactive glasses have the ability to chemically bond to bone and soft tissues when implanted in the living body.[1] The "bioactive bond" takes place through the formation of an apatite-like layer on the surface in contact with physiological fluids.[2−7] The reactions involved in this process have been described by Hench and can be summarized in five stages:[8]

Stage 1. Rapid exchange of cations such as Na^+ or Ca^{2+} with H^+ from the solution.

Stage 2. Loss of soluble silica in the form of $Si(OH)_4$ to the solution resulting from the breakage of Si−O−Si bonds and formation of Si−OH (silanols) at the glass solution interface.

Stage 3. Condensation and repolymerization of a SiO_2-rich layer on the surface depleted in alkali and alkaline earth cations.

Stage 4. Migration of Ca^{2+} and PO_4^{3-} to the surface through the SiO_2-rich layer, forming a $CaO-P_2O_5$-rich film on the top of SiO_2-rich layer, followed by growth of the amorphous calcium phosphate (CaP) by incorporation of soluble calcium and phosphates from solution.

Stage 5. Crystallization of the amorphous CaP to form a HCA layer.

Since these reactions take place on the surface, not only chemical composition but also the textural properties (pore size and shape, pore volume, etc.) play a fundamental role in the development of the HCA layer.[9−14] The sol−gel method of glass processing provides materials with high mesoporosity and high surface area, enhancing the kinetics of the apatite formation and expanding the composition range for which these materials show bioactive behavior.[15−22]

The $SiO_2-CaO-P_2O_5$ system is one of the most widely studied in the field of bioactive sol−gel glasses. Many

* Author to whom correspondence should be addressed.
[†] UCM.
[‡] USBiomaterials Corporation.

(1) Hulbert, S. F.; Hench, L. L.; Forbers, D.; Bowman, L. S. *Ceram. Int.* **1982**, *8*, 121.
(2) Hench, L. L. *J. Am. Ceram. Soc.* **1998**, *81*, 1705.
(3) Vallet-Regí, M. *J. Chem. Soc., Dalton Trans.* **2001**, 97.
(4) Hench, L. L.; Splinter, R. J.; Allen, W. C.; Greenlee, T. K. *J. Biomed. Mater. Res. Symp.* **1971**, *2*, 117.
(5) Ohura, K.; Nakamura, T.; Yamamuro, T.; Kokubo, T.; Ebisawa, Y.; Kotoura, Y.; Oka, M. *J. Biomed. Mater. Res.* **1991**, *25*, 357.
(6) Wheeler, D. L.; Stokes, K. E.; Hoellrich, R. G.; Chamberland, D. L.; Mcloughlin, S. W. *J. Biomed. Mater. Res.* **1998**, *41*, 527.
(7) Greenspan, D. C.; Zhong, J. P.; LaTorre, G. P. In *Bioceramics 8*; Wilson, J., Hench, L. L., Greenspan, D. C., Eds.; Elsevier Science: New York, 1995; p 477.
(8) Hench, L. L.; Andersson, O. In Bioactive Glasses. *An Introduction to Bioceramics*; Hench, L. L., Wilson, J., Eds.; World Scientific Publishing: Singapore, 1993; p 41.
(9) Pereira, M. M.; Clark, A. E.; Hench, L. L. *J. Am. Ceram. Soc.* **1995**, *78*, 2463.
(10) Pereira, M. M.; Hench, L. L. *J. Sol-Gel Sci.* **1996**, *7*, 59.
(11) Peltola, T.; Jokinen, M.; Rahiala, H.; Levanen, E.; Rosenholm, J. B.; Kangasniemi, I.; Yli-Urpo, A. *J. Biomed. Mater. Res.* **1999**, *44*, 12.
(12) Vallet-Regí, M.; Arcos, D.; Pérez-Pariente, J. *J. Biomed. Mater. Res.* **2000**, *51*, 23.
(13) Vallet-Regí, M.; Rámila, A. *Chem. Mater.* **2000**, *12*, 961.
(14) Greenspan, D. C.; Zhong, J. P.; LaTorre, G. P. In *Bioceramics 7*, Turku; Anderson, O. H., Yli-Urpo, A., Eds.; Butterworth-Heinemann Ltd: Oxford, 1994; p 55.
(15) Li, R.; Clark, A. E.; Hench, L. L. *J. Appl. Biomater.* **1991**, *2*, 231.
(16) Catauro, M.; Laudisio, G.; Costantini, A.; Fresa, R.; Branda, F. *J. Sol-Gel Sci. Technol.* **1997**, *10*, 231.
(17) Izquierdo-Barba, I.; Salinas, A. J.; Vallet-Regí, M. *J. Biomed. Mater. Res.* **1999**, *47*, 243.
(18) Vallet-Regí, M.; Salinas, A. J.; Román, J.; Gil, M. *J. Mater. Chem.* **1999**, *9*, 515.
(19) Martinez, A.; Izquierdo-Barba, I.; Vallet-Regí, M. *Chem. Mater.* **2000**, *12*, 3080.
(20) Balas, F.; Pérez-Pariente, J.; Vallet-Regí, M. In *Bioceramics 11*, New York; LeGeros, R. Z., LeGeros, J. P., Eds.; World Scientific Publishing: Singapore, 1998; p 125.
(21) Pérez-Pariente, J.; Balas, F.; Roman, J.; Salinas, A. J.; Vallet-Regí, M. *J. Biomed. Mater. Sci.* **1999**, *47*, 170.
(22) Pérez-Pariente, J.; Balas, F.; Vallet-Regí, M. *Chem. Mater.* **2000**, *12*, 750.

10.1021/cm011119p CCC: $22.00
Published on Web 00/00/0000 PAGE EST: 7.3

Table 1. Nominal Composition (wt %) of the Sol Glasses Synthesized

	SiO_2	CaO	P_2O_5
58S	58	33	9
68S	68	23	9

of these studies report on materials produced using thermal treatments between 600 and 800 °C to stabilize the glass.[23−27] Depending on the component ratios, these temperatures are enough to remove the organics and nitrates (when calcium is added as $Ca(NO_3)_2$), without reaching the glassy transition temperature (T_g). Therefore, these temperatures are commonly used in the final stage of the sol−gel method for this system.

However, the stabilization temperature has a very important influence on the final physical and structural characteristics of the glasses. Experiments carried out with different systems have shown that chemical structure, textural properties, and physical characteristics are highly dependent on the stabilization temperature.[28−30] The cation diffusion could be also influenced by this parameter, thus affecting the rate of HCA formation when these materials are brought into contact with the physiological fluids.

The bioactive behavior of these glasses depends on the cation diffusion for the development of an HCA layer (stages 1−3 above), and such diffusion is related to the chemical structure of the glass (cation environment). Therefore, by understanding the kinetics and activation energies of the ionic release, we can tailor the system with a specific structure for specific applications.

The aim of this work is to investigate the textural and chemical structural changes of the gel glasses with different stabilization temperatures and determine the influence of these variables on the kinetics of the ionic release.

Experimental Section

Two glasses were studied with the nominal compositions presented in Table 1. The samples were prepared by hydrolysis and polycondensation of tetraethyl orthosilicate (TEOS), triethyl phosphate (TEP), and Ca $(NO_3)_2{\cdot}4H_2O$. HCl (1 N) was used to catalyze the TEOS and TEP hydrolysis, and each reactant was consecutively added under continuous stirring. Next, the solution was introduced in a furnace and aged at 60 °C for 52 h. Drying was carried out at 180 °C for 78 h under high-humidity conditions.[31] For this purpose, the crystallizing dishes with gels were placed inside a large drying chamber with about 5000 mL of water. The dish was elevated to avoid the direct contact with water.

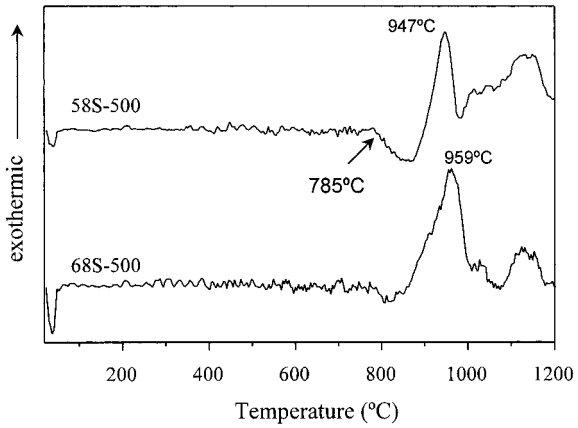

Figure 1. Differential thermal analysis (DTA) for 58S-500 and 68S-500. Glasses stabilized at higher temperatures showed similar thermograms.

Each of the dried gels was divided into four groups. Each group was stabilized at a different temperature: 500, 600, 700, and 800 °C under air atmosphere. The samples were ground and sieved. Particles ranging in size from 300 to 710 μm were selected.

XRD patterns were obtained with a Philips X'Pert diffractometer using Cu Kα radiation. FTIR were obtained with a Nicolet Magna-IR 550 (Nicolet Instruments) spectrometer. The spectra were collected by diffuse reflectance without dissolving the samples in KBr. Thermogravimetric analyses were carried out under air atmosphere and at heating rate of 5 °C min^{-1}, with a Seiko TG/ATD 320 thermobalance. N_2 adsorption isotherms were obtained using a Micromeritics ASAP 2010C instrument. To perform the N_2 adsorption measurements, the samples were first outgassed for 24 h at 150 °C. The surface area was determined using the BET method.[32] The pore size distribution between 1.7 and 30 nm was determined from the desorption branch of the isotherm by means of the BJH method.[33]

The ion solubility tests were carried out at 24, 37, and 55 °C by soaking 200 mg of glass in 200 mL of Tris buffer, buffered at pH 7.3 with hydrochloric acid and tris(hydroxymethyl)-aminomethane (THAM). Samples were exposed to the solution for 0.25, 0.5, 1.0, 2.0, 6.0, 12.0, 24.0, and 48.0 h. After soaking, the powders were removed from the solution, rapidly dried by rinsing with acetone, and placed in a drying oven at 120 °C for an hour. The calcium, silicon, and phosphorus concentration was analyzed by inductively coupled plasma spectroscopy (ICP).

Results

XRD Studies. The XRD patterns for the 58S and 68S glasses corresponded to amorphous materials, even after being heated at 800 °C (data not shown). No crystalline phases were detected.

DTA Studies. The DTA thermograms (Figure 1) showed some differences between samples 58S and 68S. As an example, Figure 1 shows the diagrams for 58S-500C and 68S-500C. Both compositions undergo an endothermic process around 785 °C (more noticeable in 58S), and several exothermic processes start at 947 and 959 °C for samples 58S and 68S, respectively.

FTIR Spectroscopy. Figure 2a shows the FTIR spectra obtained for samples 58S and 68S stabilized at 500 °C. The samples treated at 600, 700, and 800 °C

(23) Jokinen, M.; Rahiala, H.; Rosenholm, J. B.; Peltola, T.; Kangasniemi, I. *J. Sol-Gel Sci. Technol.* **1998**, *12*, 159.
(24) Arcos, D.; Ragel, C. V.; Vallet-Regí, M. *Biomaterials* **2001**, *22*, 701.
(25) Laczka, M.; Cholewa, K.; Laczka-Osyczka, A. *J. Alloys Compd.* **1997**, *248*, 42.
(26) Vallet-Regí, M.; Romero, A. M.; Ragel, C. V.; LeGeros, R. Z. *J. Biomed. Mater. Res.* **1999**, *44*, 416.
(27) Pereira, M. M.; Clark, A. E.; Hench, L. L. *J. Biomed. Mater. Res.* **1994**, *28*, 693.
(28) Araujo, F. G.; LaTorre, G. P.; Hench, L. L. *J. Non-Cryst. Solids* **1995**, *185*, 41.
(29) Li, R. Clark, A. E.; Hench, L. L. In *Chemical Processing of Adv. Mater.*; Hench, L. L., West, J. K., Eds.; John Wiley and Sons: New York, 1992; p 627.
(30) Brinker, C. J.; Scherer, G. W. *Sol−Gel Science. The Physics and Chemistry of Sol−Gel Processing*; Academic Press: San Diego, CA, 1990.
(31) Zhong, J.; Greenspan, D. C. *J. Biomed. Mater. Res. (Appl. Biomater.)* **2000**, *53*, 694.
(32) Gregg, S. J.; Sing, K. S. W. *Adsorption, Surface Area and Porosity*; Academic Press: New York, 1982.
(33) Barrett, E. P.; Joyner, L. J.; Halenda, P. P. *J. Am. Chem. Soc.* **1951**, *73*, 373.

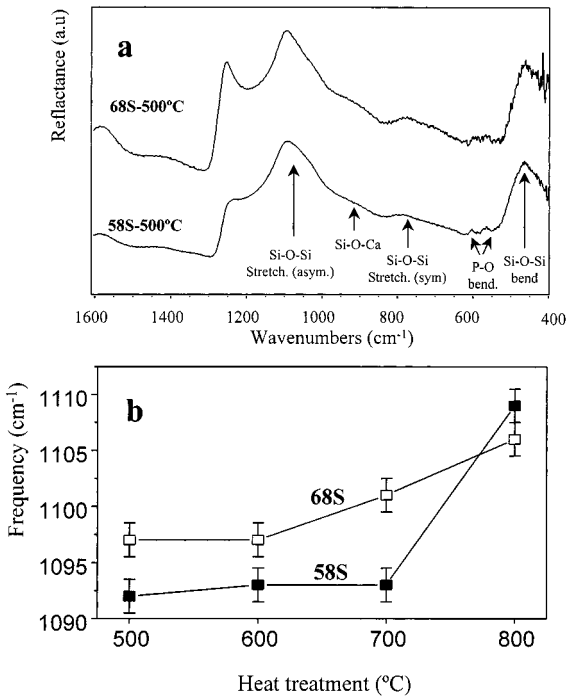

Figure 2. Infrared spectroscopy studies of the glasses synthesized. (a) FTIR spectra for 58S-500 and 68S-500. Glasses stabilized at higher temperatures showed similar spectra. (b) Asymmetric vibration frequency of Si−O−Si stretching band as a function of stabilization temperature.

showed very similar spectra. The peak at 1091 cm^{-1} is assigned to the Si−O−Si asymmetric stretching mode, while the 800 cm^{-1} vibration is associated with symmetric Si−O−Si stretching or vibration modes of the silica ring structures. The peak at 490 cm^{-1} is assigned at the Si−O−Si bending mode, while the shoulder at about 900 cm^{-1} is related to the Si−O−Ca vibration mode.[27] Finally, the double peak at 570 and 600 cm^{-1} is associated with the P−O bending mode related to the presence of crystalline phosphate in the glasses.

All of the spectra showed the peaks described above. However, differences can be noted in the position of the peak maximum (PM) at around 1091 cm^{-1}. Figure 2b shows the position of this peak as a function of the stabilization temperature for 58S and 68S sol−gel glasses. For samples treated at higher temperatures, the position of the PM is shifted to higher values. It can be observed that between 500 and 700 °C the PM shifts very little in 58S glasses. After heating at 800 °C, the frequency position of the PM increases sharply from 1092 to 1109 cm^{-1}. The same tendency can be observed for 68S glasses, but the evolution of the PM is more gradual compared with 58S glasses.

Textural Properties Study. Figure 3a,b shows the N_2 adsorption isotherms for the 58S and 68S glasses. The curves are all type IV isotherms, characteristic of mesoporous materials. The isotherms have a type H1 hysteresis loops in the mesopore range, which is characteristic of cylindrical pores open at both ends, having necks along the pores.

The d*V*/d log *D* plots show monomodal distributions centered around 8 nm for 58S-500, 58S-600, and 58S-700 and centered at 5 nm for 58S-800. However, the d*V*/d log *D* plots for 68S-500, 68S-600, and 68S-700 show a bimodal distribution centered at 5 and 10 nm, while

Table 2. Textural Parameters Obtained for the 58S and 68S Gel Glasses Stabilized at Different Temperatures (°C)

	surface area (m^2/g)	pore vol (cm^3/g)
58S-500C	175	0.533
58S-600C	172	0.534
58S-700C	173	0.532
58S-800C	88	0.170
68S-500C	282	0.478
68S-600C	273	0.464
68S-700C	263	0.437
68S-800C	220	0.346

68S-800 shows a monomodal distribution at 5 nm. The bimodal distribution can mean (a) the presence of pores with two different sizes or (b) narrowing into the cylindrical pores. Heating at 800 °C seems to remove the maxima centered at 10 nm, leaving only a narrow monomodal distribution centered at 5 nm.

The evolution of the textural properties (surface area, pore volume, and pore size distribution) with the processing temperature can be seen in Table 2. The samples 58S-500, 58S-600, and 58S-700 showed very similar surface area values of about 172−175 m^2/g, while samples heated at 800 °C showed SA values of 88 m^2/g (about 51% reduction). The 68S glasses showed higher values (about 282 m^2/g) due to the higher level of microporosity supplied by the higher SiO_2 content.[15,27,35] These values gradually decrease with the processing temperature between 500 and 800 °C from 282 to 221 m^2/g, without sharp transitions over the temperature range.

The pore volume of the glasses show a similar behavior to that of surface area. For 58S glass, the pore volume remains constant (0.53 cm^3/g) between 500 and 700 °C. The sample 58S treated at 800 °C suffers a sharp reduction of the pore volume, reaching values of 0.170 cm^3/g. For 68S glasses, the pore volume decreases gradually from 0.478 to 0.346 cm^3/g for the studied temperature range.

Cation Release Tests. The cation release tests were carried out at 24, 37 and 55 °C. Figures 4 and 5 show the cation concentration as a function of time for 58S and 68S glasses, respectively (tests carried out at 24 °C). The Ca release rate for 58S-500, 58S-600, and 58S-700 glasses (Figure 4a) show a very similar behavior. These three samples reach a maximum of 120 ppm after 1 h, remaining constant until the end of the test. Only during the first 30 min in solution can differences be appreciated between these three samples. The 58S-800 reaches the maximum of 80 ppm after 18 h, showing a slower release process.

The Si release shows a result similar to that seen with the Ca release data. Samples 58S-500, 58S-600, and 58S-700 have an identical behavior throughout the test, reaching a maximum of 60 ppm after 24 h. Even during the first 30 min, the behavior is the same for these three samples. The 58S-800 also shows a slower Si release compared with the other 58S samples throughout the test.

The plots for P release show a common feature: all of the samples show an initial P release, followed by a

(34) Brinker, C. J.; Roth, E. P.; Scherer, G. W.; Tallant, D. R. *J. Non-Cryst. Solids* **1985**, *71*, 171.
(35) Balas, F.; Arcos, D.; Pérez-Pariente, J.; Vallet-Regí, M. *J. Mater. Res.* **2001**, *16*, 1345.

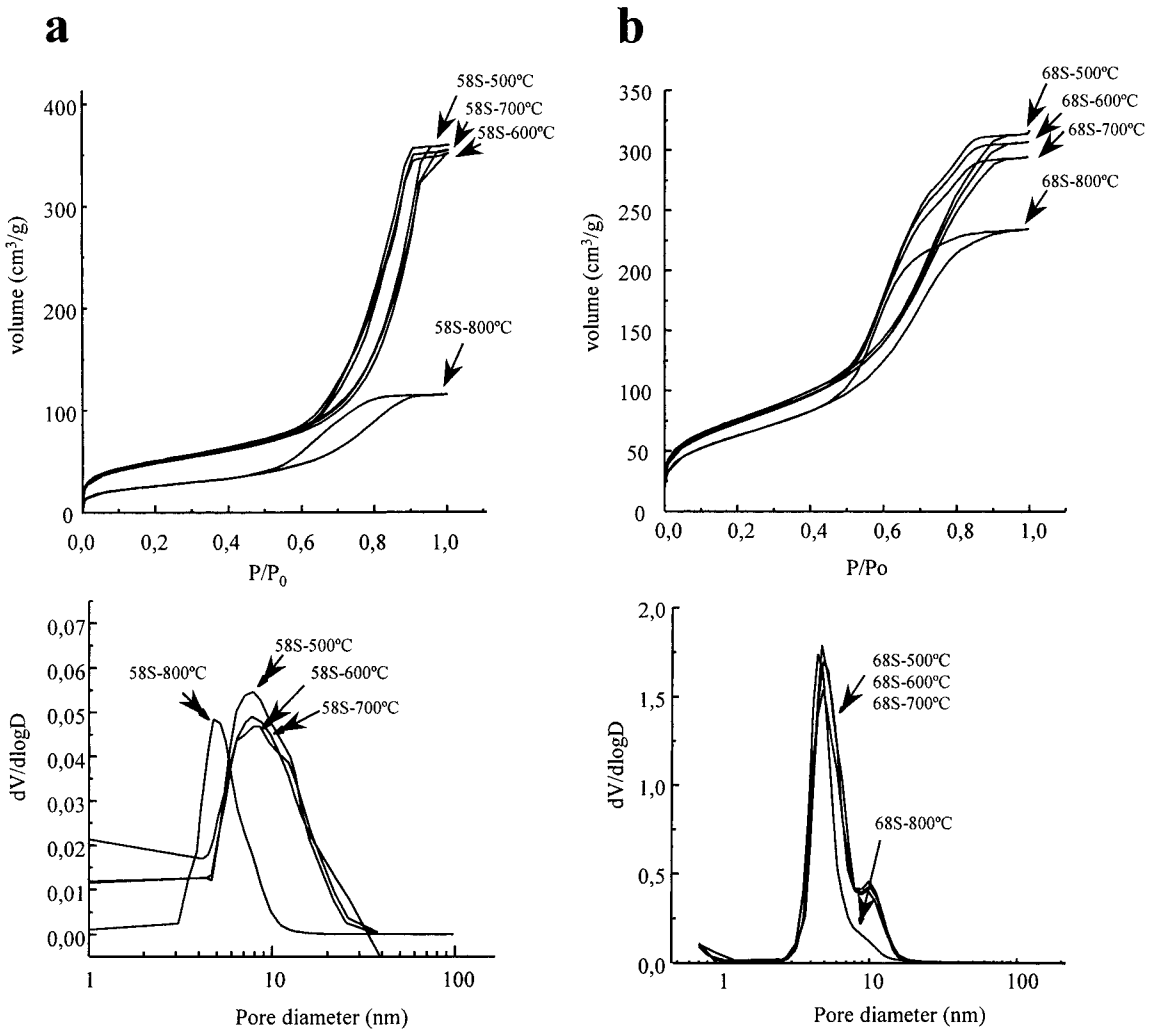

Figure 3. Isotherms (top) and pore size distribution (bottom) for (a) 58S glasses and (b) 68S glasses.

rapid decrease of phosphorus in the solution. The P is released into solution and then migrates to the surface to form a Ca−P-rich layer. 58S glasses heated at 500, 600, and 700 °C show nearly identical ionic release behavior for phosphorus, while this process seems to be slower in the case of 58-800. An explanation could be that samples heated between 500 and 700 °C release more Ca^{2+} in shorter times, and therefore phosphorus precipitated faster as calcium phosphate.

The 68S glasses show ionic release similar to the 58S (Figure 5a,b). In this case, the 68S-800 does not show big differences with respect to the other 68S glasses, and samples treated at 500, 600, and 700 °C show more gradual changes as a function of the stabilization temperature.

Calculation of Deactivation Energy (E_a). To calculate the deactivation energy for Ca and Si release, we chose the concentration measured in tris-buffer after 15 min and 6 h, respectively. Using eq 1 for an ionic diffusion model,[36] we observed that curves fit Arrhenius plots for Ca and Si in all the cases (Figure 6).

$$\ln [Ca] = \ln [Ca_0] - E_a/KT \qquad (1)$$

We obtained the E_a of Ca and Si release from the slope of the plots. E_a for P release could not be calculated, due to the very rapid precipitation of phosphorus onto the glass surface at 37 and 55 °C.

Figure 7 shows the E_a as a function of the stabilization temperature for both compositions. The E_a for Ca release gradually increase from 0.08 to 0.33 eV for 58S glasses and from 0.09 to 0.28 eV for 68S glasses. This fact shows that at higher stabilization temperature there is a higher degree of incorporation of the Ca into the silica network. Since nitrates decompose about 680 °C, they are not completely eliminated between 500 and 600 °C. We have calculated the remaining amount of nitrates by thermogravimetric analysis (Table 3). For this purpose, we have considered the mass loss between 500 and 800 °C is only due to the nitrate decomposition. The results show that a 13% of the initial $Ca(NO_3)_2$ remains in the glasses for samples heated at 500 °C. After heating at 600, 700, and 800 °C, the residual nitrates decomposed, allowing the incorporation of more Ca into the glassy matrix.

The activation energy for Si release in 58S glasses treated at 500, 600, and 700 °C is about 0,17 eV. After heating at 800 °C, the E_a sharply increase, following the same behavior than the structural density and textural parameter reduction.

(36) Holland, L. *The Properties of Glass Surfaces*; John Wiley & Sons: New York, 1964; p 142.

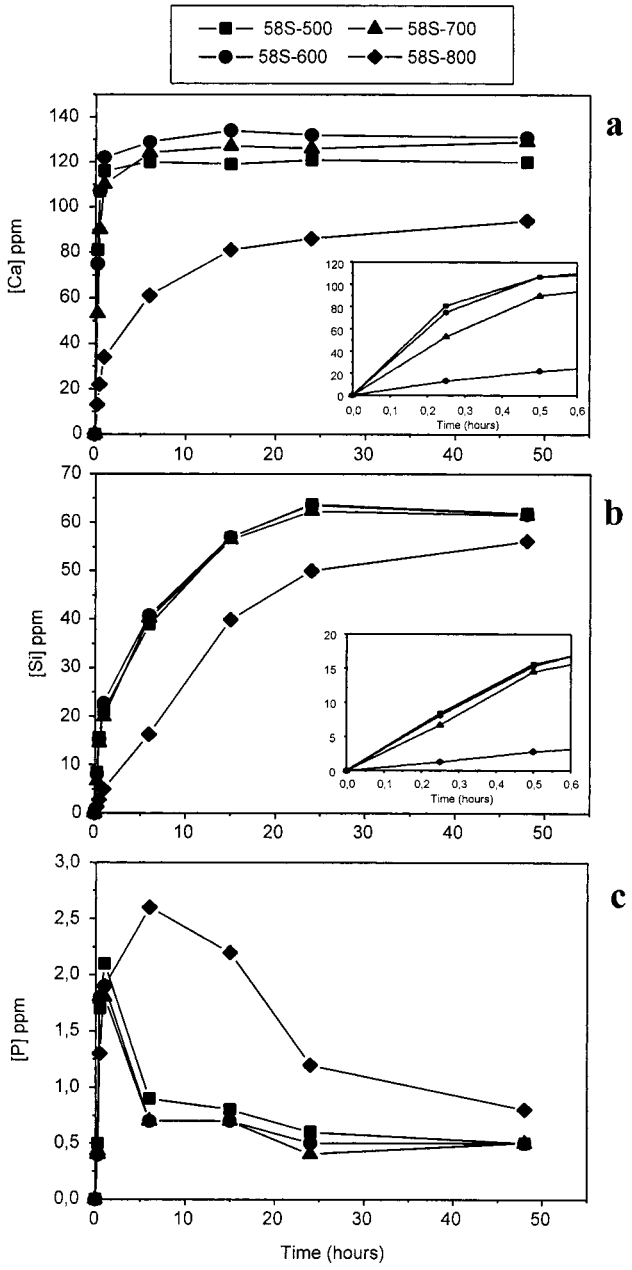

Figure 4. Ionic release as a function of soaking time in tris-buffer solution for 58S glasses: (a) Ca, (b) Si, and (c) P. Symbols corresponds to the different stabilization treatments: ■, 500 °C; ●, 600 °C; ▲, 700 °C; ◆, 800 °C. The right-down insets are *X*-axes magnifications for the first 30 min.

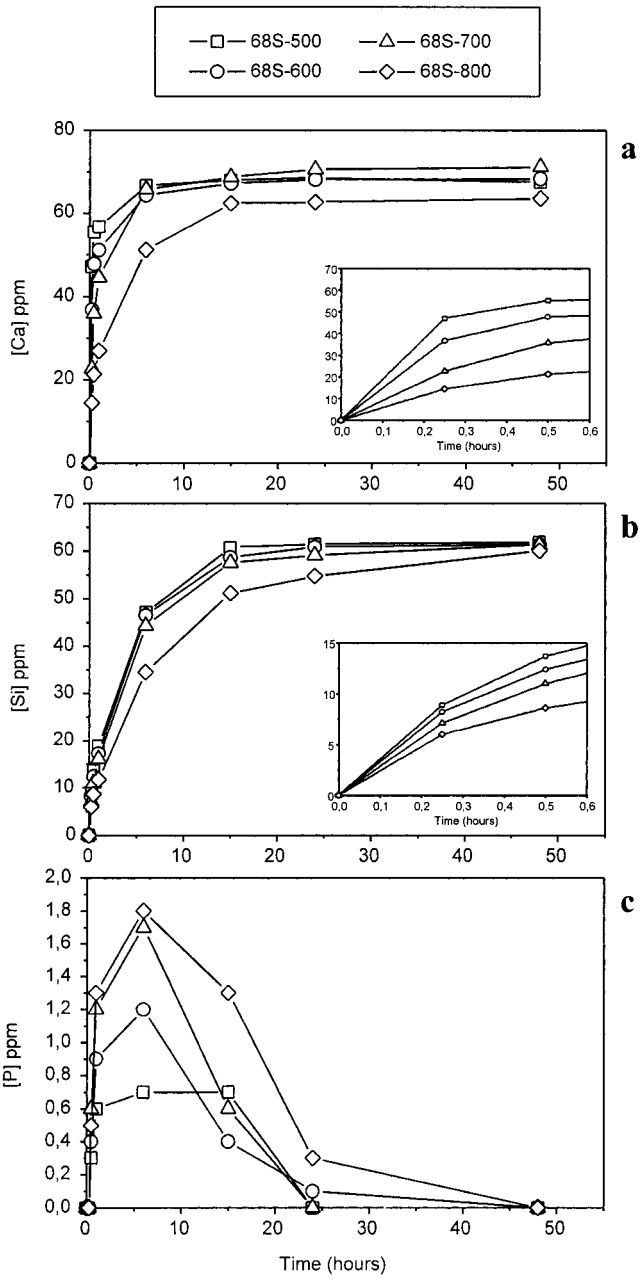

Figure 5. Ionic release as a function of soaking time in tris-buffer solution for 68S glasses: (a) Ca, (b) Si, and (c) P. Symbols corresponds to the different stabilization treatments: □, 500 °C; ○, 600 °C; △, 700 °C; ◇, 800 °C. The right-down insets are *X*-axes magnifications for the first 30 min.

The E_a for silicon release in 68 glasses also increases with thermal treatment. However, this increase is gradual from 500 to 800 °C, without sharp changes in this temperature interval.

Discussion

Differential Thermal Analysis. DTA thermograms show an endothermic peak at 785 °C. This endothermic process corresponds to the glassy transitions of the materials. At this temperature, the glasses become less viscous, the porosity is highly reduced by densification, and the gel glasses acquire similar properties to those synthesized by melting method.[34] The crystallization point (exothermic process) is 947 and 959 °C for samples 58S and 68S, respectively, confirming that all samples should be amorphous after the stabilization treatment used in this work. The higher crystallization point in 68S is due to the higher ratio network former/network modifier (SiO_2/CaO) compared to 58S.

Fourier Transform Infrared Spectroscopy. The FTIR spectra showed the characteristic peaks for sol−gel glasses with these compositions.[15,27] However, the double peak at 570 and 600 cm^{-1} related to the presence of crystalline phosphate in the glasses seems to show a contradiction with the results obtained by XRD. We suggest that, due to the high bioactivity of the composition, combined with the fact that the samples were produced in powder form (high surface area), a crystalline layer may have formed on the surface of the glass under atmospheric conditions. The nucleation of such a layer is likely to be due to reaction of the glass surface

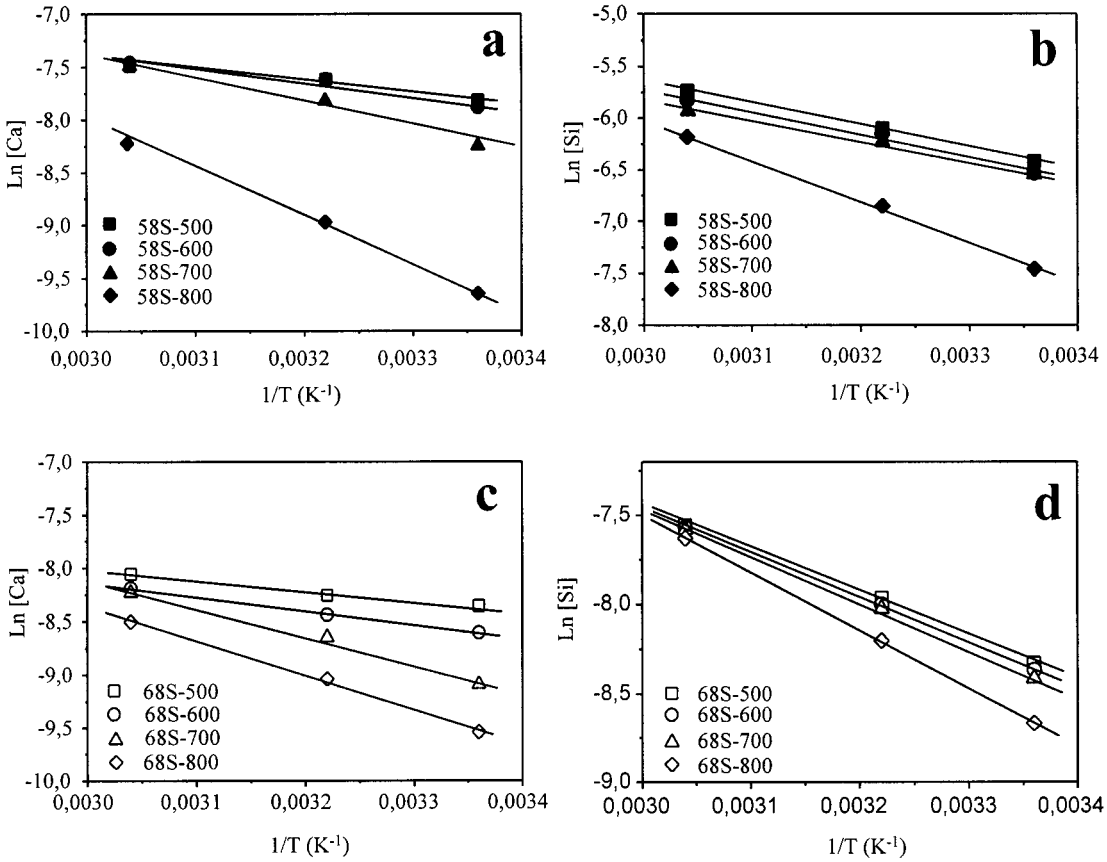

Figure 6. Arrhenius plots for (a) Ca release in 58S glasses, (b) Si release in 58S glasses, (c) Ca release in 68S glasses, and (d) Si release in 68S glasses.

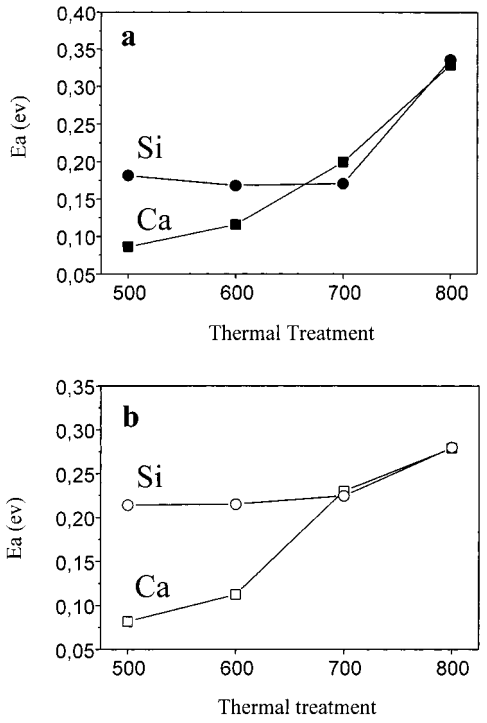

Figure 7. Activation energy for Ca and Si release processes as a function of stabilization temperature (a) for 58S glasess and (b) for 68S glasses.

and atmospheric water and Ca^{2+} ions and phosphate groups contained in the glass composition. A likely composition for this layer would be a Ca−P-rich layer that forms on the surface of bioactive glasses in contact with the physiological fluids.[15]

Table 3. $Ca(NO_3)_2$ (mol %) Remaining in the Sol−Gel Glasses after the Different Stabilization Processes

	500 °C	600 °C	700 °C	800 °C
58S	11.5	4.7	0.6	0
68S	13.7	5 0.0	0.8	0

Since the frequency of the Si−O−Si stretch peak is affected by infrared beam penetration into the sample and in that way is affected by sample density, we can correlate the Si−O−Si stretch peak shift with an increase in the structural density of our samples.[28] Following from this argument, the density of 58S seems to be stable between 500 and 700 °C. After heating at 800 °C, the density of this composition sharply increases as consequence of reaching the glassy transition temperature. This structural densification involves the reduction of the free volume of the glass by changing the conformation of the silica network, thus increasing the skeletal density. The silica network can be composed of very reactive chains or more stable condensed rings formed by SiO_4 tetrahedra. Chain conformation is often found in silicon-based gels treated at low temperatures, while three- or four-member rings are commonly found after heating between 300 and 700 °C.[37−40] When the gels are heated at temperatures close to the glassy

(37) Brinker, C. J.; Scherer, G. W. *J. Non-Cryst. Solids* **1985**, *70*, 301.
(38) Brinker, C. J.; Kirkpatrick, R. J.; Tallant, D. R.; Bunker, B. C.; Montez, B. *J. Non-Cryst. Solids* **1988**, *99*, 418.
(39) Brinker, C. J.; Brow, R. K.; Tallant, D. R.; Kirkpatrick, R. J. *J. Non-Cryst. Solids* **1990**, *120*, 26.
(40) Woignier, T.; Fernandez-Lorenzo, C.; Sauvajol, J. L.; Schmit, J. F.; Phalippou, J.; Sempere, R. *J. Sol-Gel Sci. Technol.* **1995**, *5*, 167.

transition, the structure evolves to five- or six-member rings.[41]

Study of Textural Properties. Higher stabilization temperatures reduce the surface area and the pore volume of the $SiO_2-CaO-P_2O_5$ sol−gel glasses. In this case, the densification is driven by the interfacial energy. Material moves by viscous flow or diffusion in such a way as to eliminate porosity and thereby reduce the solid−vapor interfacial area. It is interesting to remark the difference between 58S-800 and the other 58S glasses. The reduction of surface area in 58S-800C clearly shows the beginning of a densification process. In agreement with DTA analysis, this process takes place between 785 and 850 °C, and the surface area of 58S-800 (88 m^2/g) points out that the glass is not fully densified at this temperature. Therefore, we can say that 58S-800C is an intermediate state between a sol−gel glass and fully densified glass similar to those obtained by the melting method.

Although structural densification and reduction of porosity occur by different mechanisms, their behavior as a function of thermal treatment is the same for each composition. For 58S, structural density and textural parameters are stable between 500 and 700 °C and then sharply change at 800 °C as a consequence of the glassy transition process. For 68S both properties gradually change from 500 to 800 °C without sharp changes. This fact is due to the conformational flexibility of the silicon tetrahedra, which change from chains to condensed rings, and this evolution is also reflected in the textural properties.

Study of the E_a for Si and Ca Release. The changes in the structural density, pore volume, and surface area are clearly reflected by the E_a for Si release. For both compositions, there is a very close correlation between the evolution of all three parameters and the stabilization temperature. The chemical composition seems to have a fundamental role in the thermal evolution of the silicon network. In this study, the composition with higher Ca:Si ratio (58S) shows a stability interval between 500 and 700 °C, in which the silica network seems to be unaffected. Only temperatures close to the glassy transition (800 °C) lead to significant changes in the structure. However, 68S glasses are affected in this temperature interval, in such a way that 100 °C increases in stabilization temperature lead to more gradual changes in the textural and structural characteristics. All of these changes are reflected on the E_a of the Si diffusion.

The different Ca/Si molar ratios explain the differences between 58S and 68S glasses. Figure 8 is a schematic representation of these processes in our glasses. The conformational flexibility of the silicate tetrahedra allows the structural evolution from very reactive chains to more stable condensed rings. To achieve this condition, some bonds in the silica chain have to be broken before ring formation can occur, and the heat provides the energy to break these links. The presence of network modifiers, like Ca, will decrease the energy required to carry out the breaking of the bonds.[42]

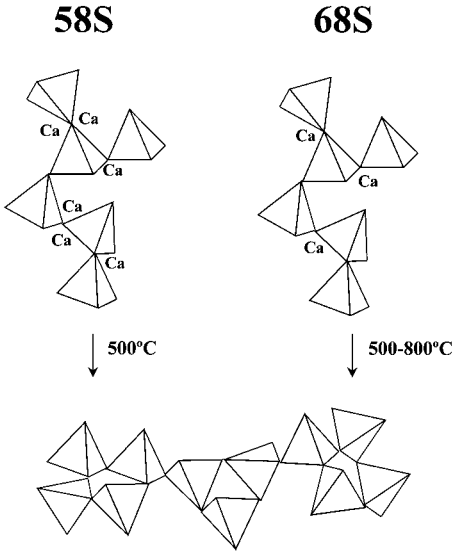

Figure 8. Schematization of the configurational changes in the sol−gel glasses. Because of the higher Ca/Si ratio in 58S glasses, 500 °C would be enough to carry out the transition from chains to rings. 68S glasses need higher temperatures due to the lower Ca/Si ratio.

The Ca:Si molar ratios are 0.60 and 0.37 for 58S and 68S, respectively. Our results show that 500 °C is enough to reach a stable structure in 58S, and only temperatures close to T_g (800 °C) change the structure, acquiring a new configuration. For 68S glasses, 500 °C is not enough to carry out the whole transition. The lower Ca content makes necessary higher temperatures to reach a stable configuration. As a consequence, between 500 and 800 °C we can observe structural and textural changes, clearly reflected on the E_a for the diffusion processes.

The E_a for Ca release gradually increases with the stabilization temperature for both samples. This fact points out a higher degree of Ca incorporation into the SiO_2 network, as a consequence of a more complete $CaNO_3$ decomposition with the thermal treatment.[43]

These results show that the stabilization temperature has a great influence on the structure, texture, and cation release. Therefore, the "in vivo" bioactive behavior will be different between the glasses. Low stabilization temperature will lead to glasses with a higher cation release rate, and resorption is expected to be faster when implanted. On the other hand, glasses treated at higher temperatures are expected to be more stable, with a similar behavior to the corresponding melt-derived composition.

Thus, it should be possible to engineer bioactive glasses in this system with a very exact rate of resorbability to treat very specific patient needs. For example, in older, osteoporotic patients in need of bone grafting, a glass stabilized at the lower temperature can be fabricated that will have a higher rate of ionic release. Given recent results that suggest that the extracts from bioactive glasses actually stimulate osteoblasts differentiation and proliferation,[44−46] these more reactive glasses could help bone regeneration in these more

(41) Brinker, C. J.; Bunker, B. C.; Tallant, D. R.; Ward, K. J. *J. Chim. Phys.* **1986**, *11−12*, 851.
(42) Doremus, R. H. *Glass Science*; John Wiley and Sons: New York, 1973; p 30.
(43) Pereira, M. M.; Clark, A. E.; Hench, L. L. *J. Mater. Synth. Process.* **1994**, *2*, 189.
(44) Xynos, I. D.; Edgar, A. J.; Buttery, L. D. K.; Hench, L. L.; Polak, J. M. *Biochem. Biophys. Res. Commun.*. **2000**, *276*, 461.

difficult cases. Similarly, for younger, more active patients, glasses can be designed to resorb more slowly, allowing the normal biological healing process to control the repair.

Conclusions

The stabilization temperature has a great influence on the structural and textural features of the $SiO_2-CaO-P_2O_5$ sol−gel glasses. The structural density increases with the temperature as consequence of the evolution from chains to condensed rings of silicate tetrahedra.

Textural and structural changes are closely correlated with the E_a for the SiO_2 dissolution, when the glass is in contact with tris-buffered solution. In these glasses, the Ca:Si ratio is very important since higher Ca concentration decreases the chains to ring transition temperature.

The higher stabilization temperature also facilitates the incorporation of Ca into the silicon network. This fact is due to the more complete decomposition of calcium nitrate remaining into the gel glasses.

By understanding the cation kinetic release and controlling the stabilization temperature, it should be possible to engineer bioactive glasses in this system with a very exact rate of resorbability to treat very specific patient needs.

Acknowledgment. This research was supported by CICYT, Spain, through research project MAT99-0466 and USBiomaterials Inc. We also thank K. McKenzie, Dr. J. P. Zhong, and Dr. J. K. West for their valuable technical and expert assistance.

CM011119P

(45) Xynos, I. D.; Hukkanen, M. V. J.; Batten, J. J.; Buttery, L. D.; Hench, L. L.; Polak, J. M. *Calcif. Tissue Int.* **2000**, *67*, 321.

(46) Xynos, I. D.; Edgar, A. J.; Buttery, L. D. K.; Hench, L. L.; Polak, J. M. *J. Biomed. Mater. Res.* **2001**, *55*, 151.